_ TN - 92 _ 039
CEBAF – NOTE – 0000
April 24, 1992
Preliminary Version

Photon Flux Computation for the HRS Spectrometers at Forward Angle

Z.-E. MEZIANI

CEBAF, Physics Division, Newport News, VA 23606

ABSTRACT

In this note we evaluate the total photon flux due to bremsstrahlung and radiative Moller scattering of the incident electron beam when crossing the high pressure gas targets. We use this flux to estimate the power deposited in the coil of the HRS spectrometer first quadrupole when set at the most forward angle and also compute the photon background that reaches the detector hut in this setting.

1. Goal and Method.

Our interest is to answer questions relevant to the high luminosity experiments in Hall A when the HRS spectrometers are in their most forward angle position.

- ♣ What is the power deposited on the coil of the front quadrupoles? Is shielding against radiation damage necessary in this case?
- ♣ What is the flux of low energy photons reaching the detector area? If this rate is high it might jeopardize the experiment. So it is important to design a shielding that will reduce the rate.

We adopted a simple approach to evaluate the photon background generated at the target. We assumed three different sources emitting photons at an angle θ_k covering a solid angle $d\Omega_k$.

- **Direct bremsstrahlung.**
- **Forward bremsstrahlung followed by Compton scattering.**
- **Radiative Moller scattering.**

We did not consider in this note the photon flux due to the subsequent decay of neutral pions produced in the target. We plan to look at this process at a later time.

1.1 Direct Bremsstrahlung

It corresponds to photons emitted at the appropriate angle in a single bremsstrahlung emission. In order to calculate this process flux we used the differential Bethe-Heitler cross section known as Formula-1BS in Reference[1], where the atomic form factor chosen is discussed in Sec.II(3) of the same reference. An exact numerical integration over the scattered electron variables provides us with a differential cross section with respect to the energy and solid angle of the emitted photon *i.e.* $d\sigma_B/d\Omega_k dk$.

$$N_{\gamma'} = F_e.N_a\Delta\Omega \int_{k_{min}}^{k_{max}=E_i} dk \frac{d\sigma_b}{d\Omega_k dk}$$

where F_e is the incident electron flux ($e^-/second$), N_a the number of scattering centers (atoms) per unit area (cm^2), and $\Delta\Omega$ the appropriate solid angle. The integration over the photon energy is performed from an arbitrary chosen lower limit (k_{min}) to an upper limit (k_{max}) usually defined by kinematics, in this case it is the end point of the bremsstrahlung energy spectrum ($k_{max} = E_i$).

1.2 Forward Bremsstrahlung followed by Compton Scattering

Photons emitted by bremsstrahlung at very forward angle in the first part of the target can undergo Compton scattering in the remaining part of the target and emerge at any angle. The large flux of photons emitted at very forward angle makes significant the large angle scattered photon flux. To calculate the photon flux due to this double step process we divided the target cell into two halfs. The first half of the target is used to evaluate the bremsstrahlung flux integrated over the angular acceptance of the full target. The second half of the target provides us with the atomic electrons necessary for Compton scattering. In this case the photon flux is obtained by convolution of two processes following the relation:

$$N_{\gamma'} = F_e.Z_a.\frac{N_a^2}{4}\Delta\Omega \int_{k'_{min}}^{k'_{max}} dk' 2\pi \int_{\theta_k^{min}}^{\theta_k^{max}} sin\theta_k d\theta_k \frac{d\sigma_B}{d\Omega_k dk} \cdot \frac{d\sigma_C}{d\Omega dk'}$$

$$k' = \frac{km_e}{k(1-cos\theta)+m_e}$$

where Z_a is number of electron per target atom, m_e is the electron mass, θ is the

Compton scattering angle and $d\sigma_C/d\Omega dk'$ is the Compton scattering cross section. Again k'_{min} is arbitrary and k'_{max} is defined as follows:

$$k'_{max} = \frac{k_{max} m_e}{k_{max}(1 - cos\theta) + m_e}$$

The angular limits depend on the target geometry and are given for specific target configuration. Other quantities are the same as in the previous section.

1.3 Radiative Moller scattering.

The radiative Moller process is the emission of photons during the electron beam scattering off atomic electrons. For the first time, we have evaluated this process with no peaking approximation. A numerical integration over the energy and angles of the scattered electron is performed leading to a differential cross section with respect to the energy and angle of the emitted photons. We used the Runge-Kutta with stepsize control integration method[2] to successfully overcome the difficulty due to the extremely peaked behavior of the integrant of the angular integration.

We started with the formula of Radiative Bhabha scattering of ref.[3] after cross checking the results with this reference, we were able to evaluate the Radiative Moller cross section by following a substitution rule.

$$\sigma(p_1, p_2, p_3, p_4) \rightarrow e^+e^-\gamma \qquad Radiative Bhabha$$

$$\sigma(p_1, -p_4, p_3, -p_2) \rightarrow e^-e^-\gamma \qquad Radiative Moller$$

where $\sigma = d\sigma_R/d\Omega_k dk$ is the differential cross section. The photon flux into the solid $\Delta\Omega$ is obtained as follows:

$$N_{\gamma'} = F_e.Z_a.N_a\Delta\Omega \int_{k_{min}}^{k_{max}} dk \frac{d\sigma_b}{d\Omega_k dk}$$

the upper limit k_{max} is quite small compared to the electron incident energy when the photons are emitted at large angle.

$$k_{max} = \frac{m_e(E_i - m_e)}{m_e + E_i - P_i cos\theta_k}$$

2. Photon Flux Calculations

We took the case of the parity experiment in Hall A to evaluate the rates of background photons. The flux of photons is calculated using the following experimental parameters:

♣ **Target**: ^{4}He Z_a=2

— length: 15 cm

— diameter: 1 cm

— pressure: 70 atm

— Surface density : $2.55 (g/cm^2) \rightarrow N_a = 38.36\ 10^{22}\ atoms/cm^2$

♣ **Target Windows**: ^{27}Al Z_a=13

— Thickness: 0.0254 cm

— Entrance surface density: $0.0686\ (g/cm^2) \rightarrow N_a/2 = 15.31\ 10^{20}\ atoms/cm^2$

— Exit surface density: $0.0686\ (g/cm^2) \rightarrow N_a/2 = 15.31\ 10^{20}\ atoms/cm^2$

The dimensions of the cell allow to calculate the angular limits for the integration of the forward bremsstrahlung in the first half of the target followed by

Compton in the remaining half of the target. The corresponding angular range in this case is: $\theta_k^{max} = 19.1mr$ and $\theta_k^{min} = 0.0mr$

2.1 Power deposited on the coil close to the beam line

The angular position of the front quadrupole coil closest to the incident beam line is $4.02° < \theta_k < 5.37°$. The distance from the pivot to the coil is about $160cm$ and the coil width is approximately $3cm$. For an overestimate of the photon flux striking the hotest section of the coil we assume the differential solid angle to be $\Delta\Omega = 3 \times 10/160^2 = 12msr$ located at $\theta_k = 4°$ for an arc of $10cm$ length. Figure 1-2-3 provides the information of the coil/cryostat assembly necessary to define the solid angle sustained by the coil quadrant closest to the incident electron beam line. Table 1 summarizes the flux of photons from different processes reaching the coil and the power deposited on the relevant coil quadrant.

Table 1

Incident energy (GeV)	average current (μA)	Direct Bremss (Hz)	Bremss. plus Compton (Hz)	Radiative Moller (Hz)	Total Flux (Hz)	Power deposited on Coil Watts
4.	100.	$0.92\ 10^9$	$20\ 10^9$	$9.4\ 10^{10}$	$1.14\ 10^{11}$	$9.6\ 10^{-2}$

It is important to point out that most of the rate is due to photons with energy which does not exceed 20MeV. The energy distribution follows dk/k leading to an average photon energy of about $5.3\ MeV$. Assuming all photons stop in the coil the power deposited is about $100mW$. We find the power deposited on the coils to be small and it will be easy to shield and prevent any radiation damage.

2.2 Flux of photons in the detector hut

Now we turn to the computation of the flux of photons entering the spectrometer. In this case the experimental parameters are more accurate. $\Delta\Omega = 8msr$ and the central angle is $\theta_k = 12.5°$. A good fraction of these photons undergoes Compton scattering in the middle section of the HRS spectrometer dipole magnet. The scattering angle necessary to reach the detector area is about 45°. As an approximation we evaluate the rate of photons of energy above $500keV$ reaching the detector area by Compton scattering on a target of thickness equal to $100\mu m$ of Iron ($0.0787\ g/cm^2$, $8.5\ 10^{20} atoms/cm^2$).

Table 2. Rates estimate for the flux of photons at $\theta_k = 12.5°$ from the the different processes we discussed and the rate at the detector location

Table 2						
Incident energy (GeV)	average current (μA)	Direct Bremss (Hz)	Bremss. plus Compton (Hz)	Radiative Moller (Hz)	Total Flux (Hz)	Flux in Detector area (Hz/sr)
4.	100.	$10.5\ 10^6$	$11.1\ 10^9$	$2.9\ 10^{10}$	$4.0\ 10^{10}$	$0.68\ 10^6$

3. Conclusion

From the previous computations summarized in Table 1. and 2. we find that running at high luminosity with the HRS in the most forward position does not pose any major problem. A shielding that stops photons up to 21 MeV energy is sufficient to decrease the power deposited on the coils to negligible levels for any possible radiation damage. The rate over the full detector area is not critically high and should not be of serious concern. This is mainly due to the large bend angle of the HRS dipole. We point out that we did not consider in this note the photon flux due to the decay of neutral pions produced during the passage of the beam in the target. This process might not be significant at 4 GeV incident beam energy but might become relevant at larger incident beam energies. The evaluation of this process and an update of this note will be available soon.

REFERENCES

1. H. W. Koch and J. W. Motz, Rev. Mod. Phys. 31, 920(1958)

2. W. H. Press, B.P. Flannery, S. A. Teukolsky and W. T. Vetterling, Numerical Recipes, The art of scientific computing, Cambridge University Press

3. S. M. Swanson, Phys. Rev. 154 1601(1967).

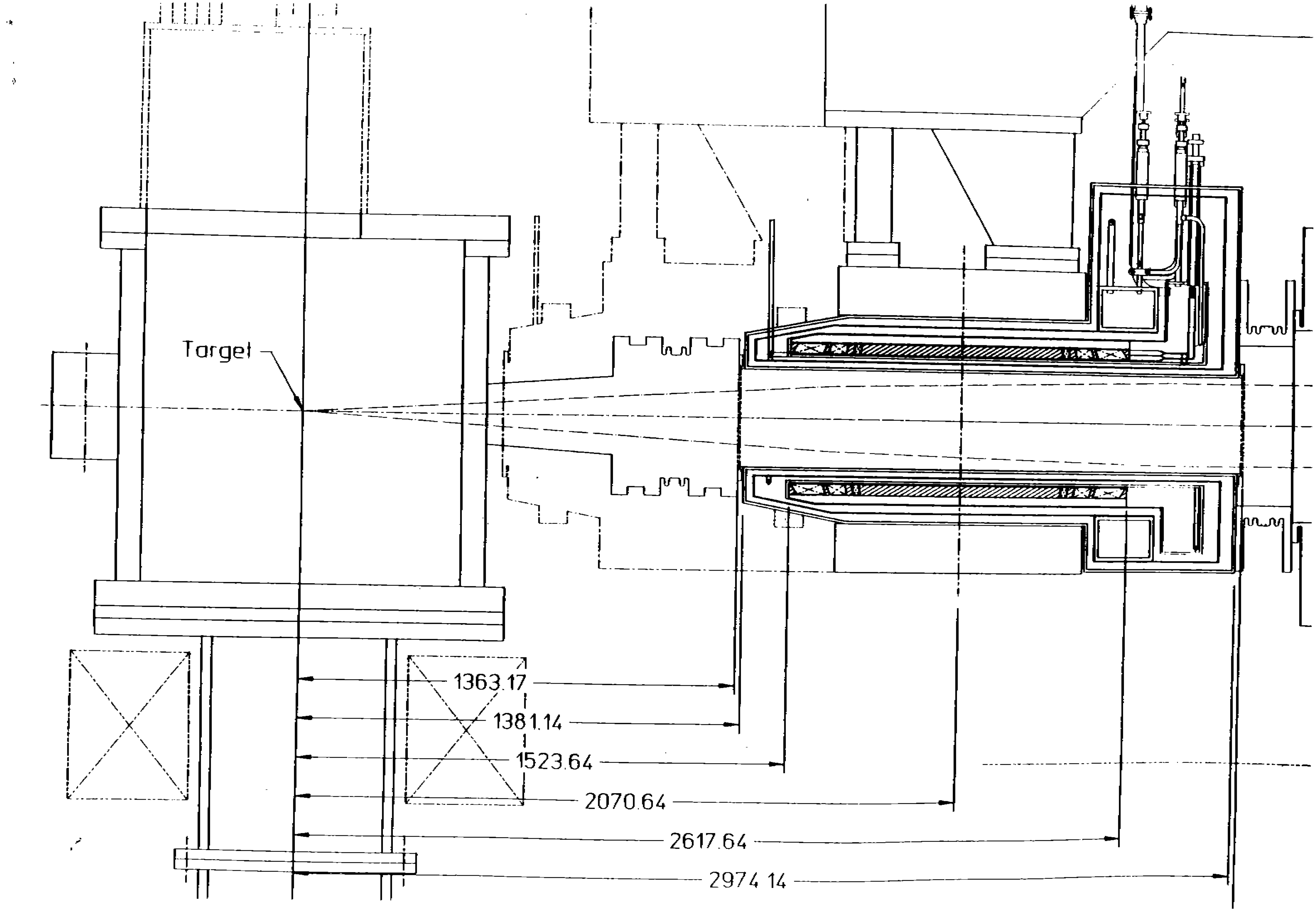

FIGURE 1

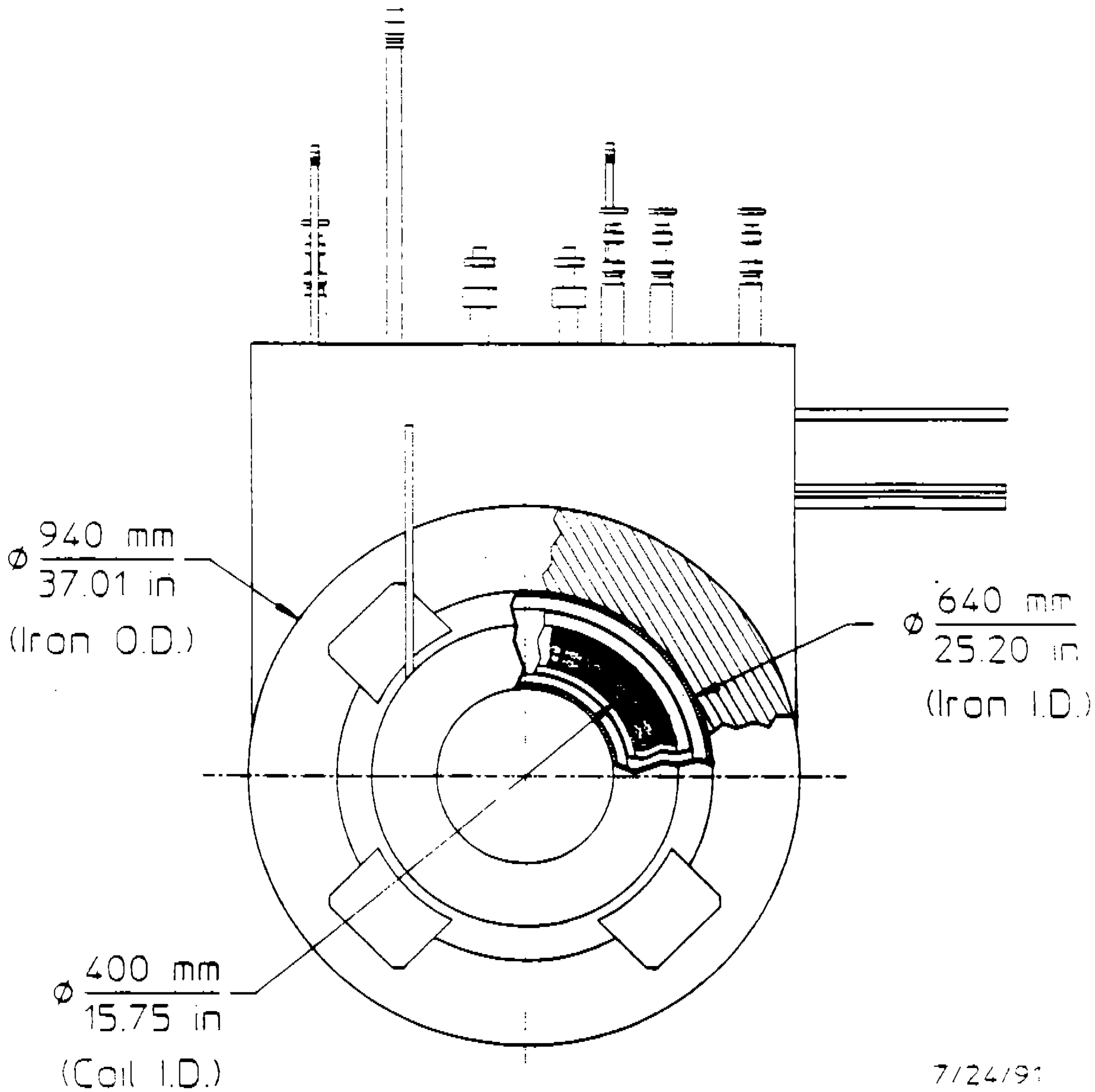

Coil/Cryostat Assembly: Front View

Figure 2

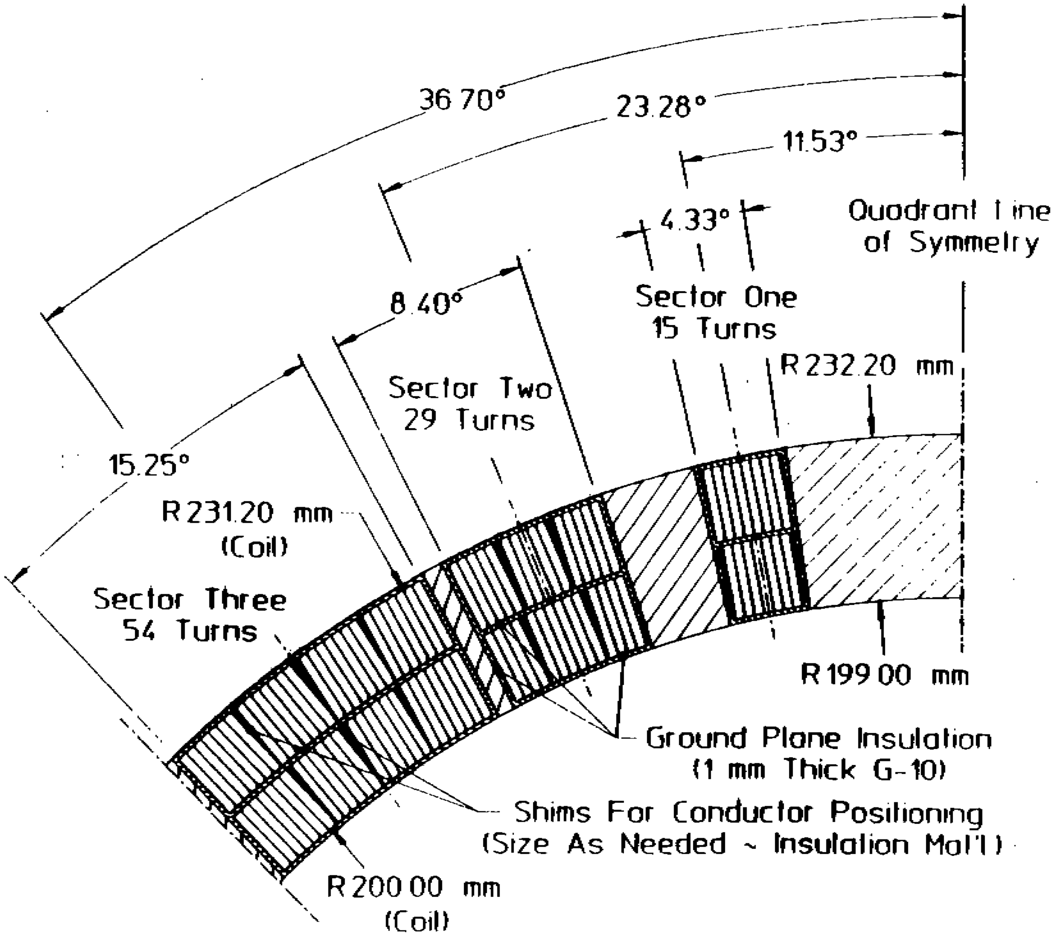

7/23/91

Coil Quadrant Cross–Section

Figure 3